

Pattern Formation During Anodic Etching of Semiconductors

H. Föll and J. Carstensen

Institute for Materials Science, University of Kiel, Kaiserstr. 2, 24143 Kiel, Germany

The current burst model asserts that current flow through anodically dissolving semiconductor electrodes is localized in space and time. The only relevant parameters of the model are probability functions for current “on” and “off”. Interactions between current bursts in space and time account quantitatively, or at least qualitatively, for a wealth of pattern formation phenomena observed on semiconductor electrodes that are classified as oscillations in time and space (= pore formation). The paper reviews these electrode oscillations in the light of the current burst model.

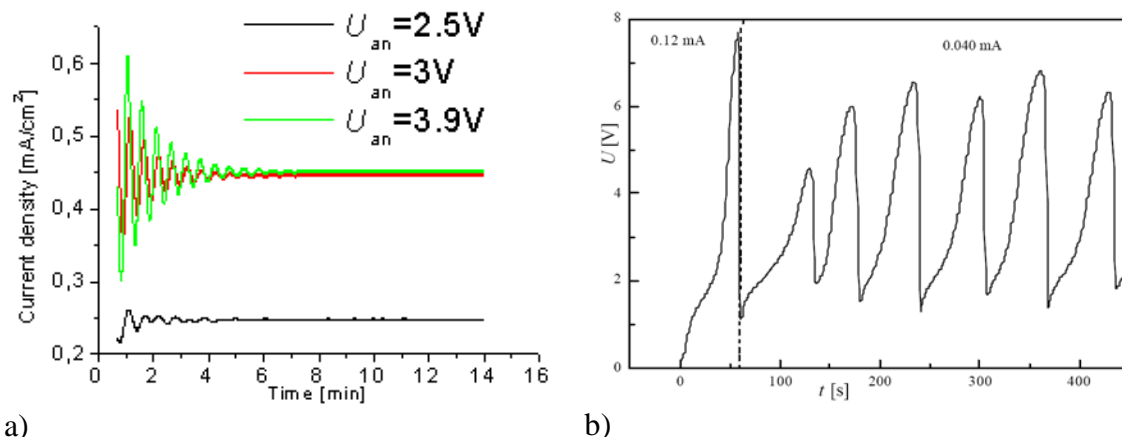
1. Introduction

A number of self-organization or pattern formation processes are observed during the electrochemical dissolution of single crystals of semiconductors such as Si, Ge, III-V's like InP and GaAs, and II-VI's like ZnSe, cf. (1) and references therein. Many of these pattern formation phenomena can be described as current oscillations in time or space. Oscillations in time of the external current flowing through an electrode in an electrochemical system driven under potentiostatic (i.e. constant external voltage) conditions are nothing new. For silicon anodes they have been described extensively, cf. for example, (2 - 6) and the references therein. Voltage oscillations in time have also been found during galvanostatic (i.e. constant external current) experiments in Si (cf. (7)); more recently a number of papers also address voltage or current oscillations in InP (8 - 11). Self-induced oscillations in time of the open-circuit potential in Si were observed, too (12); and many more observations on the topic “oscillations in time” have been reported.

The word “oscillation” in the context of this paper refers to some repetitive behavior of a relevant quantity in time or space, not necessarily always well-behaved and sinus like, and is seen as an expression of some self-organization. Oscillations thus might be sustained (the amplitude stays constant for a reasonable time span); “explosive” (cf. (1)), meaning that the amplitude increases until the system “explodes”; damped; or hidden. Hidden oscillations are present, for example, in some porous structures that are produced by dissolution. An oscillating current flows through every pore but with random phases. The total external current then adds up to a rather constant value, hiding the intrinsic oscillatory behavior.

Fig. 1 gives two illustrative examples for oscillations in time as found with p-type Si at HF concentrations of a few wt. %, cf., e.g., (2 - 6, 1, 13). While the question has been raised if sustained oscillations, i.e. oscillations with no damping at all and thus always relying on some intrinsic synchronization mechanism, actually exist in this context (the Palaiseau group around Chazalviel and Ozanam recently denied this (14)), here we consider all oscillations, including heavily damped ones as shown in Fig. 1a), to be an expression of some self-organization process. Oscillations obviously express an intrinsic time constant of the system, typically in the range of seconds or milliseconds, that is far

larger than time constants that can be associated with the chemical reactions at the atomic scale or with the electron – hole dynamics in the bulk of the semiconductor.



a) b)
 Fig. 1 Examples of oscillations in time found with Si electrodes at low HF concentrations around 0.1 wt%. a) Damped current oscillations at various potentiostatic conditions. b) Voltage oscillations at galvanostatic conditions (0.04 mA/cm^2). Initiating these oscillations needs a “nucleation” period of 0.12 mA/cm^2 as shown.

Oscillations of the current in space as exemplified in Fig. 2 have not yet been addressed extensively in the literature, in contrast to current oscillations in time. The self-organized pore crystal in InP shown in Fig. 2a) (after (15)) formed because at the place of a pore (dark region) the localized current flow has dissolved InP to a depth of $> 300 \mu\text{m}$ while in between the pores the current density was zero or at least very low. The current distribution on the sample surface thus is periodic in two dimensions; the resulting pore single crystal (with defects like dislocations and stacking faults) must be interpreted as the result of a self-organized current oscillation in space. Figs. 2b) – c) show pore arrangements that can be interpreted as damped current oscillations in space. Fig. 2c), while apparently showing a random distribution of pores in Si, actually shows a frustrated crystal, trying at the same time to be cubic and hexagonal. This leads to no correlations in the angular distribution with respect to next neighbors but to a clear correlation for second-next neighbors as evidenced by the Fourier transform in the inset. Even Fig. 2d), where the pores and thus the current distribution shows no directly obvious periodicity, is not completely random with respect to pore sizes and pore distances. Pore arrays formed by current oscillations in space clearly express an intrinsic length scale of the system, typically in the $50 \text{ nm} - 5 \mu\text{m}$ range that is far larger than length scales that can be associated with the length scales of chemical reactions at the atomic scale, or even with the typical thickness of intermediate product layers like SiO_2 .

There are many different expressions of pattern formation in time and space during the anodic dissolution of semiconductors. The so-called “current burst” (CB) model of the authors has gone a long way towards modeling these effects and this paper will briefly review the results.

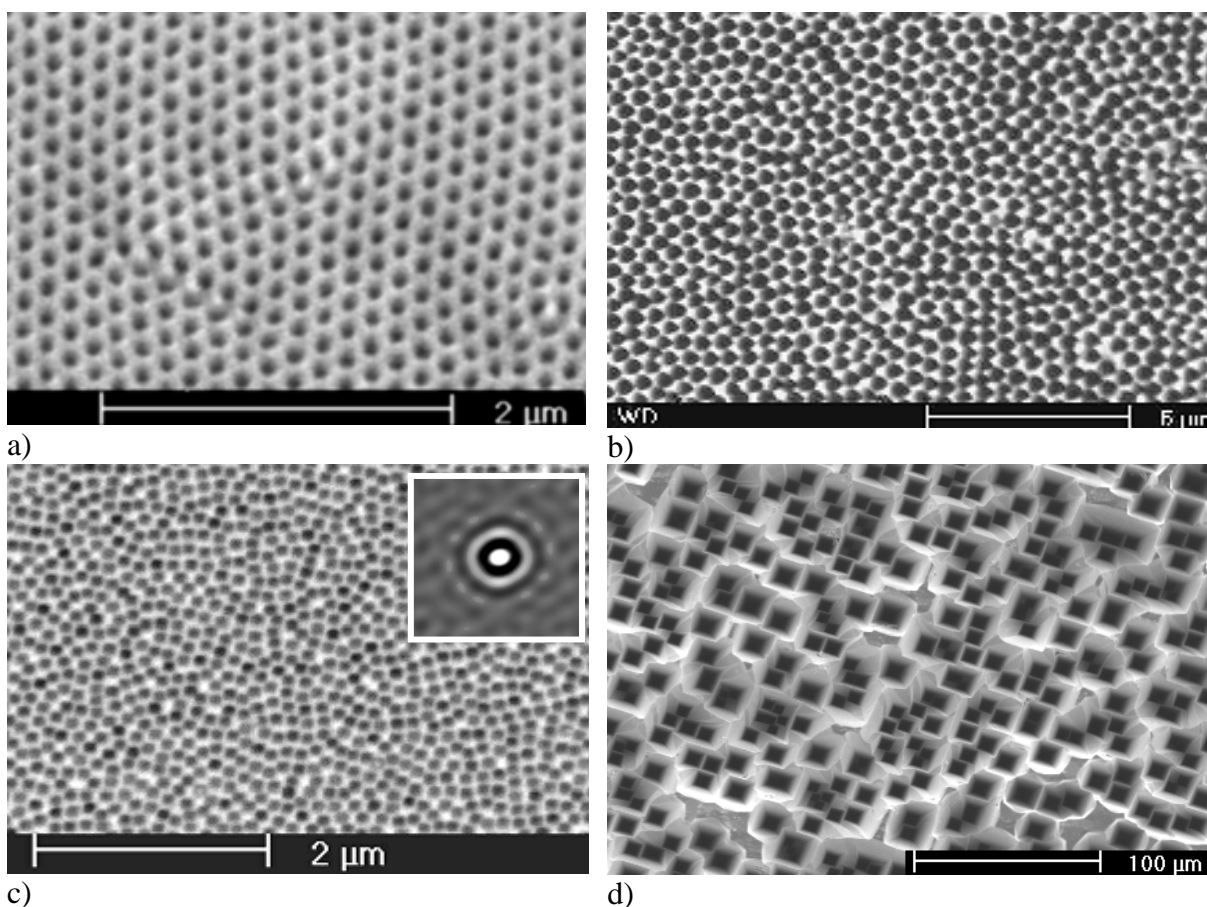


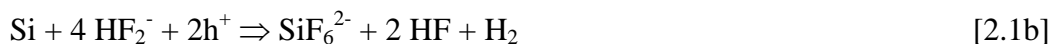
Fig. 2 Examples of current oscillations in space. a) Pore single crystal in {100} n-type InP. b) Short range order (“damped oscillation”) for pores in {111} n-type Si. c) Frustrated pore crystal in {100} n-type Si (see text for details). d) Random pore distribution in {100} n-type Ge obtained in an HCl electrolyte (note the much larger scale).

2. Essentials of the Current Burst Model

In conventional electrochemistry the current flow through an electrode is usually perceived as continuous and with smooth changes in time and space. This is schematically depicted in Fig. 3a) for current flow through a Si anode covered with a thin oxide. The CB model introduces a new and completely different paradigm, claiming that current flow in many cases consists of “current bursts” or charge transfer events at the interface that are localized in time and space as schematically depicted in Fig. 3b). In essence, this will happen whenever the reactive interface is covered with a barrier layer or, in other words, whenever there is a reaction that passivates the interface. The simplest case, concerning Si electrochemistry, is the formation of an oxide layer by the potential-driven tetravalent reaction



This reaction dominates at high potentials and competes with the divalent direct dissolution dominating at low potentials (Eq. 2.1b). In addition there is purely chemical oxide dissolution (Eq 2.1c).



Moreover, an oxide-free Si surface will eventually become covered with hydrogen. Hydrogen is considered to passivate the Si surface to some degree, just as Cl^- ions passivate InP surfaces, OH^- species passivate Ge surfaces, and so on. As far as the CB model is concerned, the only parameter of interest is the average field strength needed to overcome a passivated surface, i.e. the average field strength needed to initiate or nucleate current flow locally. Since passivation layers are never absolutely uniform, the field strength E is not uniform either and current flow starts locally at “weak” points. In the case of a thin oxide layer as shown in Fig. 3b), the local oxide thickness is the decisive parameter. The term “average” field strength indicates that initiation of the current flow or the nucleation of a CB has a stochastic component.

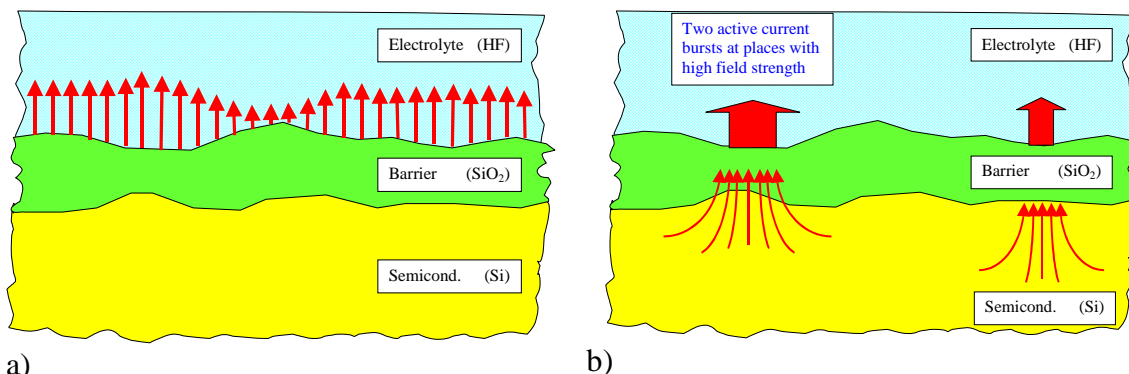
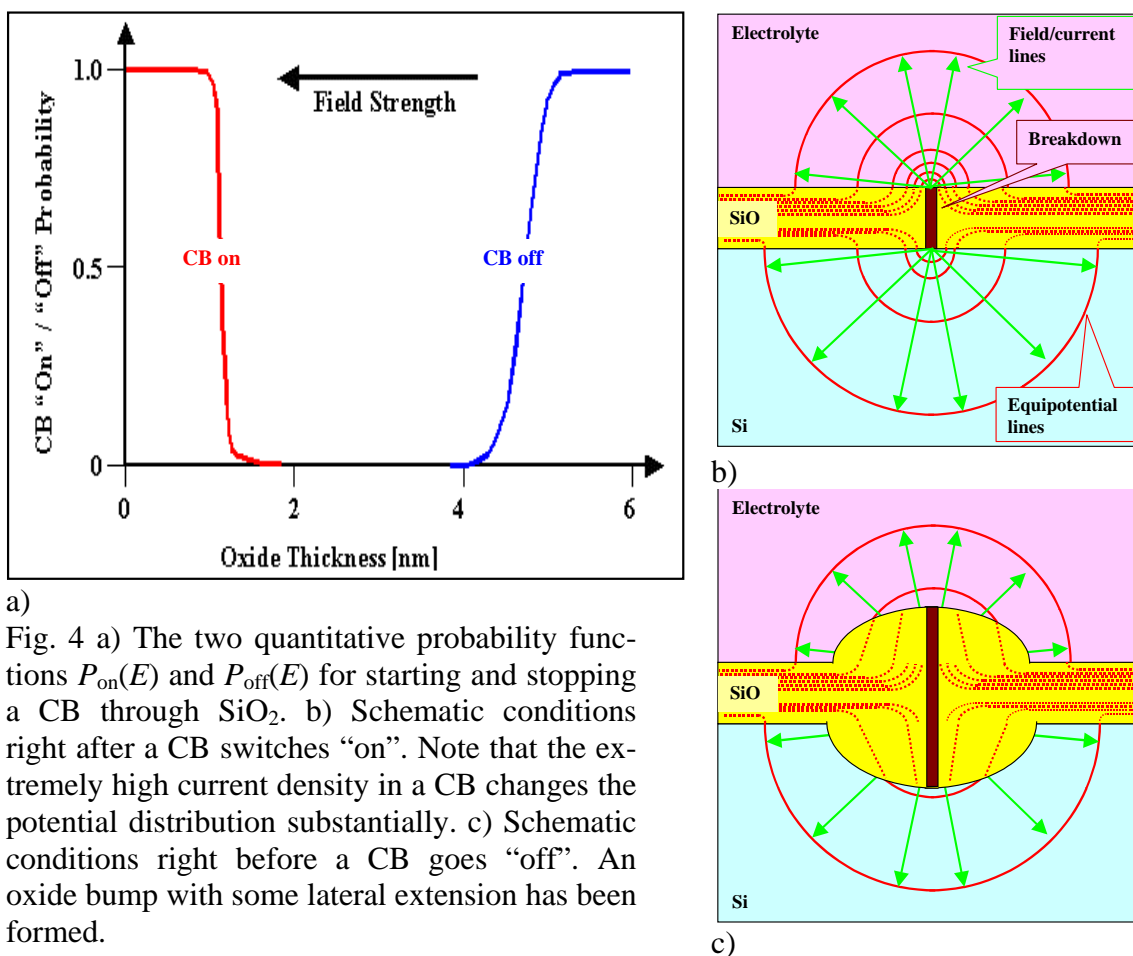


Fig. 3 Two ways of modeling current flow through an electrode covered with a barrier layer; here Si oxide. a) The “normal” paradigm. The current flow is homogeneous in time and space. b) The CB paradigm. The current flow occurs as a localized current burst that has a beginning and an end.

The first major ingredient of the CB model is thus the probability function $P_{\text{on}}(E)$ for initiating a CB. For SiO_2 as barrier this function has been fully quantified. Fig. 4 shows $P_{\text{on}}(E)$ as used for quantitative modeling the current flow through an oxide covered Si (7). While the exact shape of $P_{\text{on}}(E)$ for SiO_2 has been determined to some extent by fitting experimental data to the quantitative model described below, it also has to agree with what is known about the electric breakdown of oxides and is thus far from being a “free” parameter or function. For the general case $P_{\text{on}}(E)$ has not yet been quantified for all kinds of barrier layers but this is not essential for what follows. The essential point is that there is a stochastic component in the initiation of local current flow.

The second major ingredient of the CB model asserts that after initiation of a CB at some “pixel” (x, y) and time t , the chemical reactions tied to the current flow always tend to make the current flow more difficult and after some time actually stop it. Once more this process is most easily seen for Si dissolution. Under most conditions oxide formation will sooner or later increase the local oxide thickness (Fig. 4c) and thus decrease the local field strength E . Accordingly, a probability function $P_{\text{off}}(E)$ as shown in Fig. 4a) is needed to describe this. Again, $P_{\text{off}}(E)$ must conform to what is known about breakdown events; generally requiring some hysteresis in going from “on” to “off”.



The two probability functions $P_{\text{on}}(E)$ and $P_{\text{off}}(E)$ constitute the CB model and are all that is needed for applying the CB model to Si electrode oscillations in time. In a more general version these two functions have more variables than just the local field strength, for example the crystallographic orientation $\{hkl\}$ of the interface in question.

Anything else that will be needed to fully describe what is happening on the electrode is not part of the CB model but part of the specifics describing the physico-chemical system in question. This includes the possible reactions at the interface, local potential drops around an active CB because of series resistances, locally varying dissolution rates because of local roughness, local pH changes induced by the localized reactions, diffusion or transport of various species from and to the interface, and so on and so forth.

The CB model, however, introduces something new and alien to the “continuous” model as illustrated in Fig. 1a): the system now has intrinsic time constants and additional intrinsic length scales. Time constants, for example, are expressed as the (average) frequency of CBs occurring in a “pixel”, which in turn is given by the sum of the (average) “on” and “off” times of a CB. Length scales tied to CBs are the size of a CB or the resulting oxide bump (typically nm, scaling with the layer thickness) and the domain size of phase-coupled CBs to be discussed shortly. It goes without saying that the CB model thus introduces some basic ingredients indispensable when dealing with oscillations in time and space. Of course, the continuum model has intrinsic scales, too, in particular for semiconductor electrodes. Most prominent is the width of the space charge region d_{SCR} and the radius of curvature needed to induce electronic breakdown of the space charge region for a given potential. These two doping-level dependent length scales are the most impor-

tant length scales for many (but not all) pores found in semiconductors; they qualify as relevant system parameters like the others mentioned above also within the CB model. It is also important to realize that quantities like current density and potential lose their classical meaning. In the CB model they are just averages over local values that may deviate substantially from the mean. The current density in an active current burst, for example, can be orders of magnitude larger than the average current density, while the local potential around an active CB can be substantially lower than the applied potential due to ohmic losses.

3. Oscillations in Time Calculated with the Current Burst Model and Predictions for Pore Formation

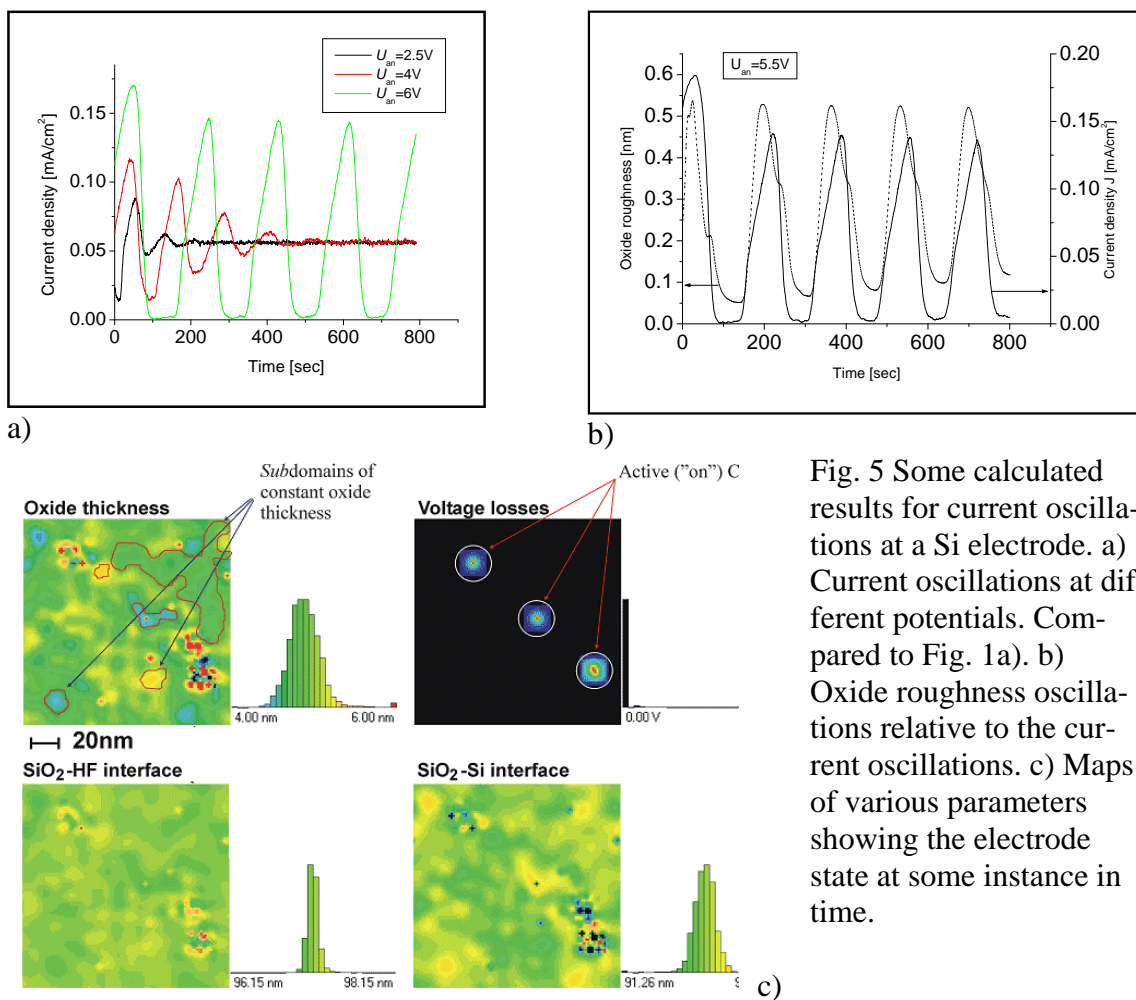


Fig. 5 Some calculated results for current oscillations at a Si electrode. a) Current oscillations at different potentials. Compared to Fig. 1a). b) Oxide roughness oscillations relative to the current oscillations. c) Maps of various parameters showing the electrode state at some instance in time.

Current and voltage oscillations occurring at a p-type Si electrode for low HF concentrations and current densities have been modeled with the CB model in great detail and with very good agreement to experiments; details are given in (7). The two probability functions as shown in Fig. 4a) are the only model specific inputs; everything else like the local oxide dissolution rate for rough interfaces, the potential drop in given electrolytes, and a synchronization mechanism are either given by the system parameters or emerge without being programmed into Monte-Carlo simulations of the dissolving anode. Note that the CB model is the only model so far that faithfully reproduces voltage oscillations

at galvanostatic conditions, something that competing models (needing far more assumptions; (16, 5, 17)) cannot do at present.

Fig. 5 shows a few calculated features resulting from Monte-Carlo simulations; note that parameters like surface and interface roughness as a function of time can be calculated; the results agree with the (limited) numbers of in-situ measurements made so far.

While isolated CBs are not phase correlated, phases start to synchronize as soon as a critical CB density (akin to a critical external current density) is reached. The synchronization mechanism is an intrinsic feature of the CB model; Fig. 6 shows the basic mechanism. If a CB is nucleated sufficiently close to an older one, it will not have to produce as much oxide as an isolated one before it turns itself off. Its behavior in time is thus correlated to what its neighbors are doing, and that induces the formation of phase-correlated domains that produce the externally measured current oscillations. The corresponding correlation length depends on many parameters, the most important ones being the external current density and the HF concentration (and thus the oxide dissolution rate). More details are provided in (7).

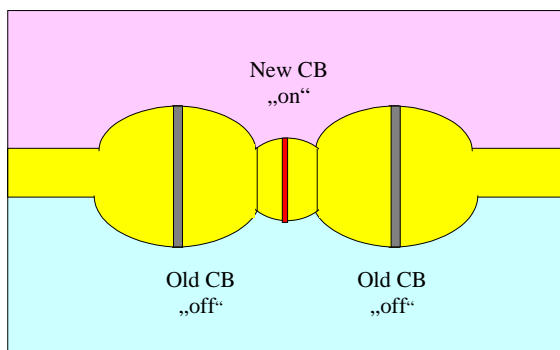


Fig. 6 Basic synchronization mechanism inherent in the CB model. See text for details.

Here we only note a general feature of the CB model: interactions between CBs in space cause correlations in time, i.e. phase coupling. Correlated CB domains, described by some correlation length, will result.

In most cases of anodic Si dissolution (and, by inference, anodic dissolution of other semiconductors), several dissolution mechanisms act in parallel. In the case of silicon, logic dictates that local divalent direct dissolution of the oxide-free interface must precede dissolution via tetravalent oxidation and subsequent oxide dissolution, since the latter process turns off the CB. Active current bursts, in a way of speaking, thus compete with oxide formation that eventually turns them off. Under conditions where only divalent dissolution is prevalent, active CBs compete against hydrogen passivation of the surface and concentration changes of chemical species promoting (e.g. HF) or opposing (e.g. reaction products) current flow because of diffusion limitations. Generalizing a bit more, we note that a CB is more likely to nucleate on a freshly etched surface than on a (hydrogen) passivated one, or on patches with a thin oxide layer compared to those with a thicker one. Since a freshly etched surface will passivate with a certain time constant, and the oxide layer thickness in an HF bearing electrolyte will decrease with time, the nucleation probability of a new CB in a given pixel will also depend on the “history” of that pixel.

In other words, CBs may also interact in time. What is likely to happen now at time t in any given pixel depends on what has happened before at time $t - \Delta t$ on that pixel and Δt is now a variable entering the probability function. We may distinguish two basic interactions besides no interaction: the probability of nucleating a new CB in certain pixel some time Δt after an old one expired might be smaller or larger than the probability on the

“average” surface. The first case is likely to occur when a bare, not yet passivated surface is left after a CB turned off, the latter one when a solid oxide bump is produced. What happens in either case is that interactions in time produce correlations in space - or pores, in other words!

We are now in a position to make some predictions with respect to pore growth under conditions where the CB model holds:

1. Nanopores or macropores result from the two basic CB interactions in time.
2. There is always a stochastic element in pore formation. This allows modelling some pore growth without knowledge of details.
3. The current in individual pores oscillates in most cases even under galvanostatic conditions.
4. Pore growth occurs with some intrinsic time constants tied to the CB model.
5. Some of these time constants are $\{hkl\}$ dependent, and this determines the pore crystallography.
6. A pore growing system has additional intrinsic length scales (besides space charge region width and so on) tied to CB length scales that might be expressed in the pore geometry.

In what follows, these 6 predictions will be discussed and verified with some examples from pore etching experiments.

4. Pore Formation in Semiconductors and the Current Burst Model

4.1 Nanopore and Macropore Formation in p-Type Silicon

Anodic dissolution of low-doped p-type Si in aqueous HF bearing electrolytes produces either straight macropores in $\langle 100 \rangle$ or $\langle 113 \rangle$ directions with diameters in the μm range, or a random network of nanometer-sized pores properly called micropores but usually referred to as nanopores. Macropores typically form at low current densities and HF concentrations and thus low potentials, nanopores form at high current densities just below the so-called PSL-peak (PSL = porous Si layer) marking the transition from pore formation to electro polishing; for details refer to (2, 18). The dominating dissolution mechanisms are direct dissolution in the macropore case, and direct dissolution plus some oxidation in the nanopore case.

This is not easily explained in conventional models but easy to understand with the CB model. If direct dissolution with almost no oxidation is observed at small current densities, the few CBs needed to carry the average small current are slightly more likely to nucleate on pixels where a previous one just expired because passivation has not yet occurred. It is easy to show that this interaction in time eventually leads to a clustering of CBs as shown in Fig. 7. In essence, a phase-correlated domain with a domain current density that is close to the density at the PSL peak forms at some areas, while almost no current flows through the rest of the sample. The CB domain then “digs” itself into the depth of the sample and a macropore is formed. The domain formation process takes some time, and this is what one observes if macropores are generated “randomly”, i.e. without nuclei defined by lithography, Fig. 14b) shows an example. Note that the CB model explains why macropores under these conditions form in the first place and why they need a pronounced nucleation time. The CB model does not claim, however, to predict the complete geometry and morphology of the pores formed; for this one needs to take more system parameters into account. The CB model does predict, however, that the

pore size tends to be close to the domain size and in particular that it cannot be smaller than a correlation length or domain size; it thus gives indications on how to control this size. This insight allowed identifying conditions for the growth of large macropores in highly doped n-type Si (19), something previously believed not to be possible.

In contrast, at high current densities close to the maximum in the PSL peak, the surface needs to be densely covered with CBs, each of which produces a nano-sized pore by direct dissolution followed by some oxidation (20), see Fig. 7b). The formation of nano-sized “oxide plucks” inside the nanopore formed by a CB will terminate the local current burst but a new one needs to be formed immediately somewhere else because the average current density (about proportional to the number of active CBs) needs to be constant under the typical galvanostatic conditions. Nucleation of new CBs is most likely just above the oxide bump as illustrated in Fig.7b) because these areas are not yet fully hydrogen passivated. A random network of nano-sized pores results, with a geometry that is also determined by the necessity to stop the current flow (= extinguish a CB) as soon as a growing nanopore approaches an existing one to a “nanodot” distance, i.e. as soon as the distance between pores become so small (nm range) that quantum effects decrease the carrier density to a level where the Si becomes effectively an insulator. Note that the CB approach to the formation of nanoporous layers answers open questions left by the only other model invoking only nanowire effects (21), e.g., why nanoporous layers have never been observed in other semiconductors.

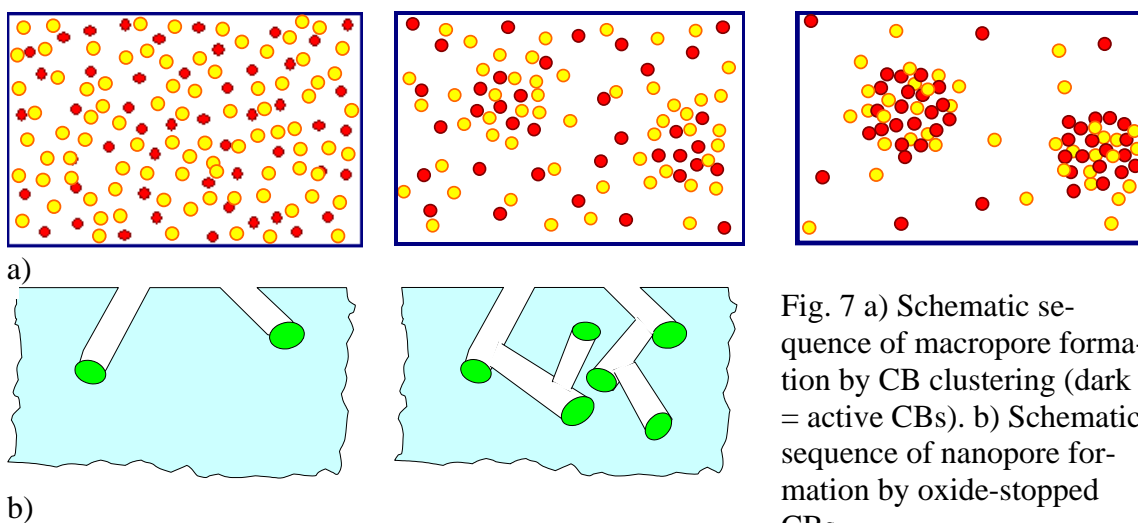


Fig. 7 a) Schematic sequence of macropore formation by CB clustering (dark = active CBs). b) Schematic sequence of nanopore formation by oxide-stopped CBs.

4.2 Modeling the Growth of Crystallographic Pores in InP and GaAs

Anodic dissolution may produce two completely different kinds of pores: “crystallographic” or “crysto” pores, growing in a preferred crystallographic direction ($\langle 110 \rangle$ and $\langle 113 \rangle$ in the case of Si and Ge, $\langle 111 \rangle$ in the case of III-V’s), and current line or “curro” pores, growing in the direction of the current flow or perpendicular to equipotential planes, for details see (22). Crysto pores may also have faceted cross-sections and tend to branch. It is possible to model the three-dimensional growth of crysto pores with the CB model quite closely, using only two numbers describing the probability for continued growth of a main pore (originally nucleated at the surface) or the growth of various generations of side pores issuing from pore walls. Fig. 8a) illustrates the three-dimensional Monte Carlo model and the geometry of the growing pores; details can be found in (23).

The simulations even revealed some fine structures such as small amplitude oscillations of the pore density with depth, cf. (24), that were actually present in experimentally obtained images but not previously recognized, and otherwise reproduced observed pore arrangements quite faithfully. Fig. 8b) shows an example for GaAs.

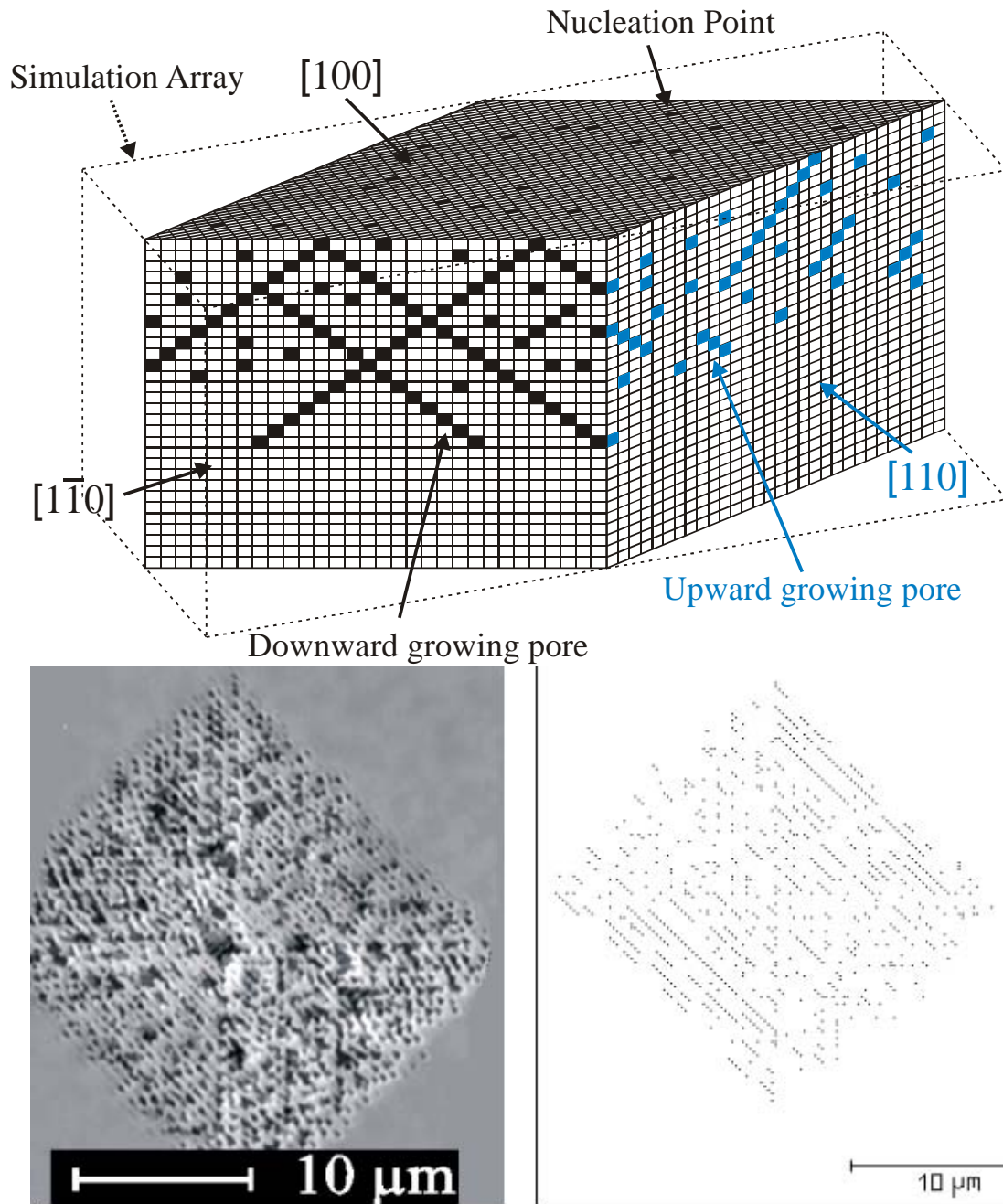


Fig. 8 a) Structure and geometry of the three-dimensional Monte Carlo model used for simulating the growth of crystallographic pores in III-V semiconductors. b) Left: Picture of a pore arrangement formed on the surface of a GaAs crystal by repeated branching of the main pore growing downward. Pore branches that grow towards the surface produce the observed structure. Right: Simulation of this pore arrangement with the CB model.

It is rather clear that many of the more complex pore structures observed, often with strongly branching crystal pores, follow the same basic stochastic principles with just somewhat more complex probability functions for continued straight growth or branching.

4.3 Current Oscillations in Individual Pores

As shown in chapter 3, some interaction in space between CBs will produce current oscillations under potentiostatic conditions rather naturally. At least for some types of pores in Si these conditions also prevail inside the pores and it can be assumed that this is also true for other semiconductors (where the precise nature of the various dissolution reactions are not yet clear). However, oscillations of the current flowing through individual pores will not be noticed externally as long as the phases of these oscillations are not correlated. With typically millions of pores growing on a standard 1cm^2 sample during anodization, the total sum of oscillating random-phase currents provides for a rather constant external current with little noise. A constant external current under galvanostatic or potentiostatic conditions thus cannot rule out “hidden” oscillations in the pores.

Current oscillations in a pore may also express themselves in pore diameter oscillations as shown in Fig. 9; for details see (22, 25). The staggered tetrahedra observed for III-V pores growing in $\langle 111 \rangle$ directions, or the staggered octahedra observed for Si pores growing in $\langle 100 \rangle$ directions, are easily explained by the CB model invoking some $\{hkl\}$ dependent probability functions, see (22, 26) and what follows. A particular remarkable feature of these pores in InP is that their basic geometry is observed in electrolytes like HCl, NaCl dissolved in water, or NaOH solutions (27, 28), proving beyond doubt that the detailed chemistry of the dissolution cannot account for these phenomena. All that matters is that some conditions for turning CBs “on” and “off” exist.

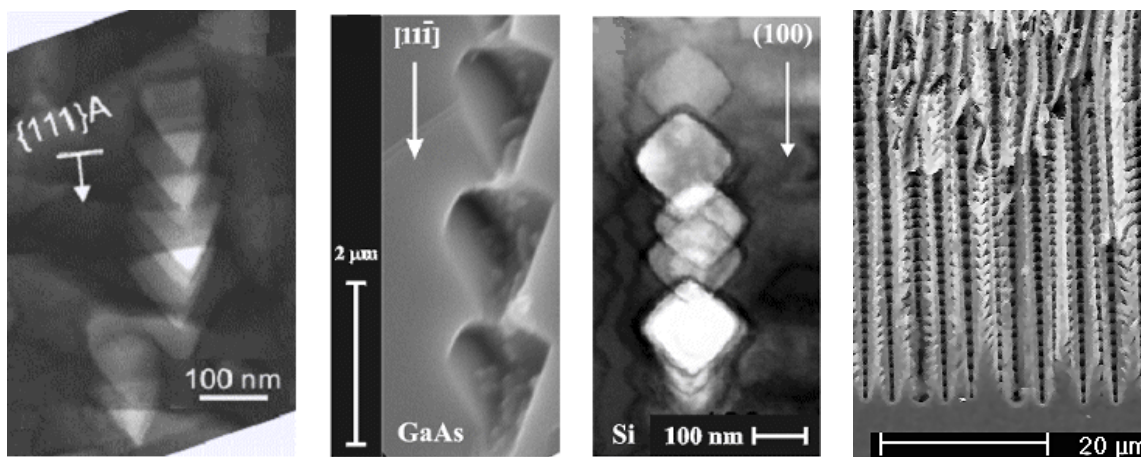


Fig. 9 Some TEM observations of pore diameter oscillations leading to staggered tetrahedra in InP or GaAs, staggered octahedral in Si or more complex structures in Si (far right).

If etching conditions are changed in such a way that the (average) diameter of the pores in Fig. 9 would become larger than their average distance, the pores are now forced to grow with constant diameter determined by the thickness of the wall between neighboring pores that scales strictly with the space charge region width d_{SCR} . As soon as these dimensions are reached, the semiconductor between the pores is now effectively an insulator that cannot sustain current flow (or, more precisely, only “leakage” currents). It is

thus inert and will not be dissolved. In this case pores tend to be of the current-line type and neighboring pores interact in space with interesting consequences: the phases of the oscillating currents in individual pores may now synchronize.

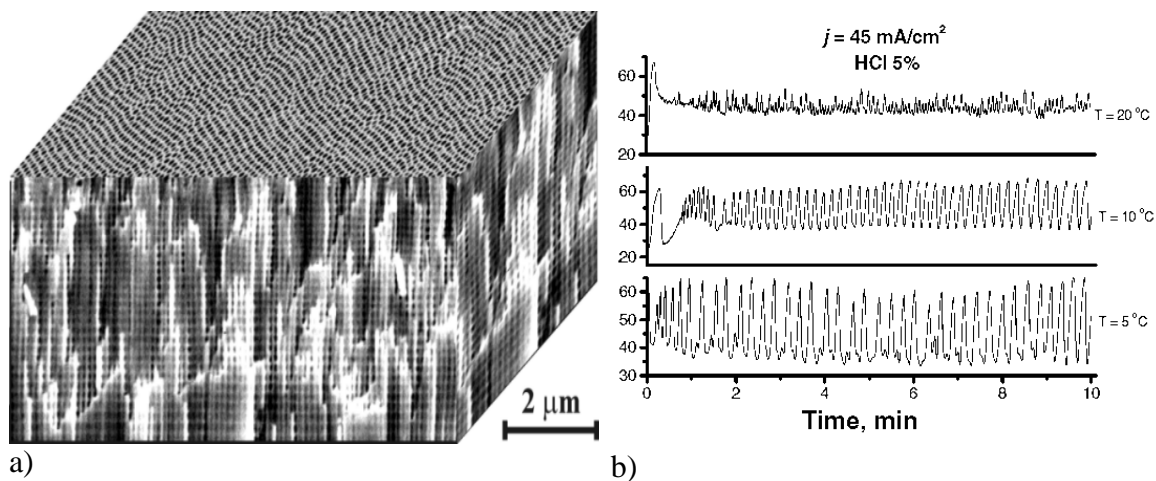


Fig. 10 a) Three-dimensional InP pore crystal formed galvanostatically, exhibiting synchronized diameter oscillations. b) Voltage oscillations coupled to synchronized diameter oscillations for different temperatures T . Decreasing T increases synchronization.

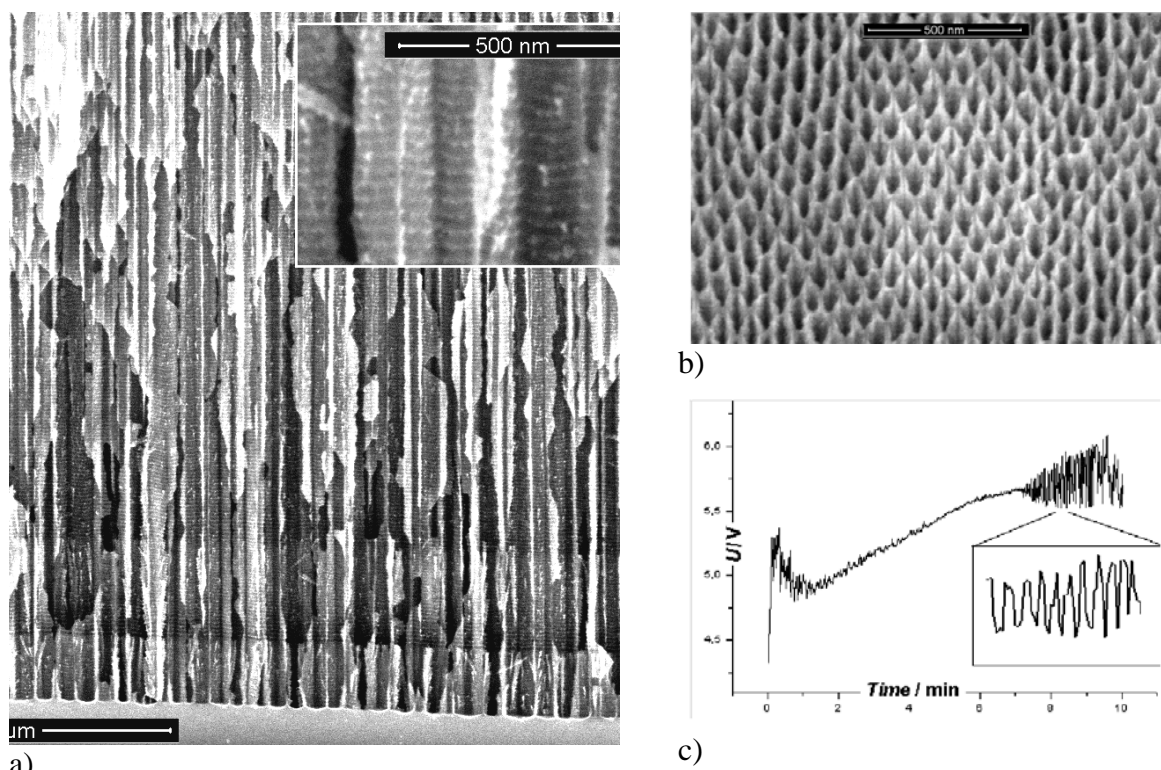


Fig. 11 a) Three-dimensional Si pore crystal formed galvanostatically, exhibiting synchronized diameter oscillations (the inset shows details). b) Surface of the sample, showing pore crystal formation. c) Voltage oscillations coupled to the synchronized diameter oscillations.

External current oscillations should result if the correlation length or domain size of phase-correlated pores is comparable and large enough. For galvanostatic control, the

voltage must oscillate since this is the only way to keep the current constant. This is exactly what has been observed consistently in InP (again for wildly different kinds of electrolytes), Si and GaP; Fig. 10 and Fig. 11 show examples, for details refer to (8, 15, 22).

4.4 Pore Growth Occurs With Intrinsic Time Constants.

Time constants or frequencies related to the oscillatory “on” – “off” behavior of CBs are an integral part of the CB model, and one could expect that some aspects of pore formation bear witness to this. Of course, the rest of the system also expresses time constants τ , e.g. $\tau = L^2/D$ (L = some diffuse length, D = diffusion coefficient) or $\tau' = RC$ (R = resistance, C = capacity) which are of importance. The oscillating current in pores already expresses a time constant of the CB model but there are more effects than that. Generally, given the non-linear nature of the CB model, one might expect that superimposed periodic external disturbances at frequencies that scale with the internal (CB) frequencies of the system might produce strong non-linear effects. This is what one observes on occasion, e.g. when trying to modulate the pore diameter by modulating the etching current. Naïve views of pore etching claim that the diameter should change directly proportional to the current - but this is rarely found, cf. (29, 30). While much could be said to this point, we restrict ourselves to just one striking example to what might be loosely termed “chaotic resonance” in Fig. 12. The only difference between the etching conditions of the two sets of pores shown was a 20 % amplitude modulation of the current in Fig. 12b) with a frequency of 33 mHz. Modulations with some other frequencies in the low mHz range had no effect. While systematic experiments to this point are still scarce, we consider the above prediction to be met.

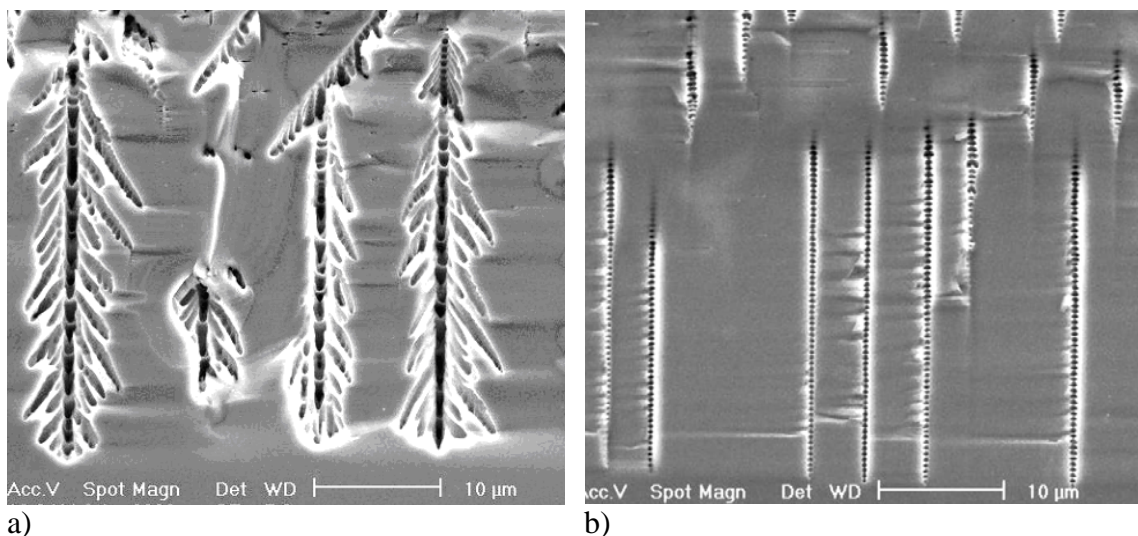


Fig. 12 Effect of modulating the etching current. a) Macropores in n-type Si etched with constant current. b) Macropores in n-type Si etched by modulating the otherwise constant etching current somewhat (20 %) with a frequency of 33 mHz. All other conditions were unchanged.

4.5 Crystal Orientations and the Current Burst Model

The electrochemically-induced growth of crystallographically oriented pores often expresses anisotropies of the dissolution rate, sometimes but not always similar to purely chemical anisotropic dissolution. For example, {111} planes in Si are most stable (“stopping planes”) and strong differences of the dissolution rates for {111A} and {111B} planes in III-V semiconductors are found during anodic dissolution. While this is similar to anisotropic chemical etches, it still needs to be explained - in particular because all these semiconductors also have pore growth modes where there is no anisotropy at all. The issue becomes even more complex when it is taken into account that crystal pore growth in Si proceeds either in $\langle 100 \rangle$ directions or in $\langle 113 \rangle$ directions if the available $\langle 100 \rangle$ directions are too steeply inclined, e.g. in {111} oriented samples.

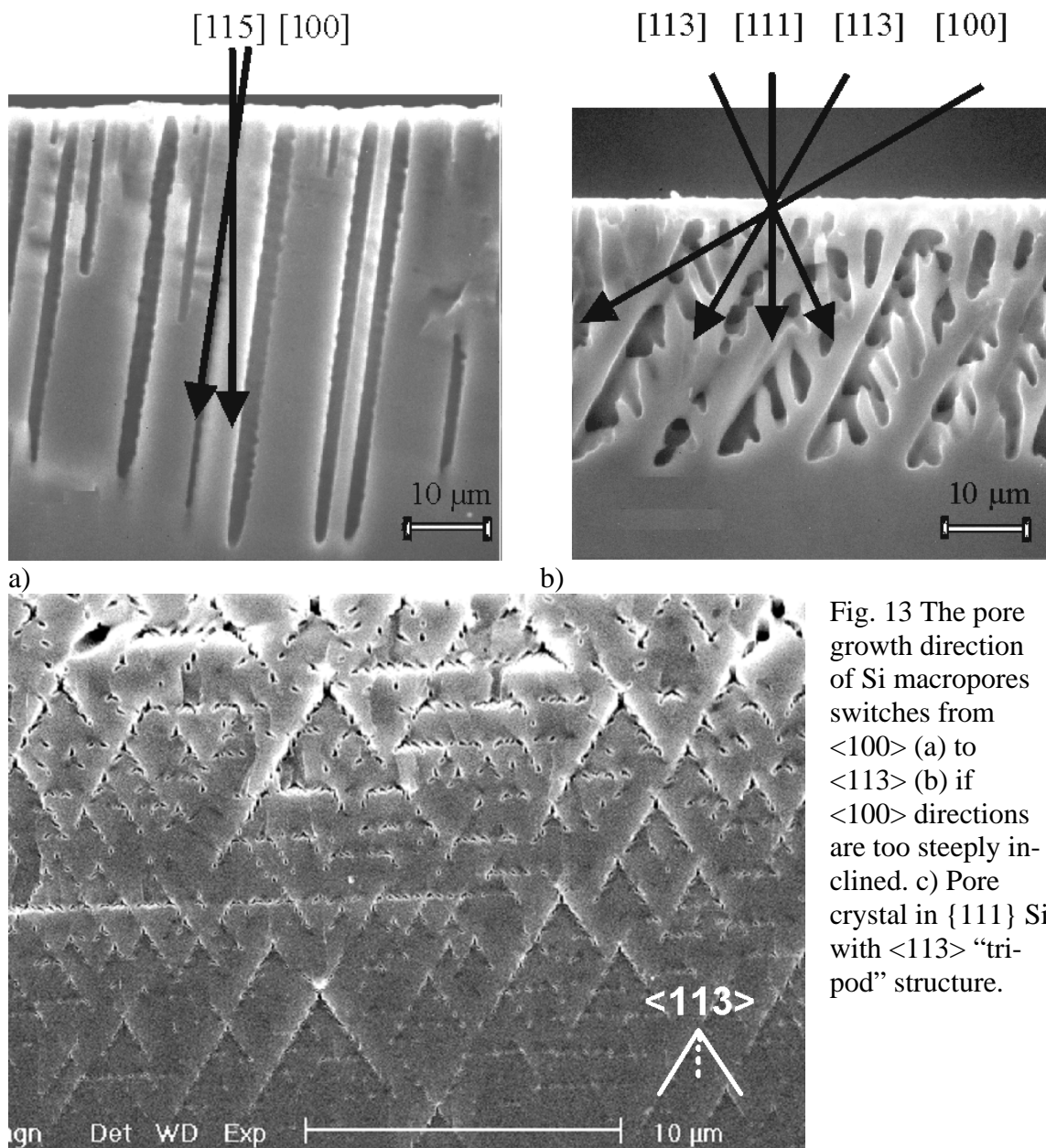


Fig. 13 The pore growth direction of Si macropores switches from $\langle 100 \rangle$ (a) to $\langle 113 \rangle$ (b) if $\langle 100 \rangle$ directions are too steeply inclined. c) Pore crystal in {111} Si with $\langle 113 \rangle$ “tripod” structure.

This is an amazing and quite unpredicted behavior of pores; no attempt outside of the CB model has been made to explain this feature. It would be premature to state that the CB model can explain this peculiar behavior in detail; it does however provide the basic ingredients necessary towards an explanation. Pore growth by necessity demands that most of the current flows through the pore tip. If that is the case, we have already established that current flow occurs in an oscillating manner by synchronized domains of CBs. A new cycle of CBs thus will nucleate most likely on that part of the tip that has the highest field strength (plane parallel to the surface “looking” towards the potential source) and the lowest degree of passivation ($\{100\}$ plane, not necessarily parallel to the surface). The $\{100\}$ planes have the slowest passivation kinetics and thus meet both criteria if the corresponding $\langle 100 \rangle$ direction is not too steeply inclined. If it is, $\{113\}$ planes with the second-slowest passivation kinetics take over as the major dissolution planes, being the best compromise between the two conditions. The observed branching geometry is also explained in this way. The $\{hkl\}$ dependent time constants for passivation thus determine parts of the pore crystallography. While no direct measurements of these time constants exist, the hypothesis given above is generally consistent with what is known about the role of $\{113\}$ planes in Si etching.

Similar arguments hold for pore growth directions found in other semiconductors. Moreover, the self-induced or externally triggered growth mode changes from crystal pores to curved pores (or the other way around; see (31) for details) or, in other words, the complete loss of any crystallographic “information” in pore growth, also fits into this general picture.

4.6 Length Scales of the CB Model and Pore Geometry

The basic geometry of pores in semiconductors is mostly tied to system length scales; most prominent in this respect is the space charge region width d_{SCR} . The two major length scales provided by the CB model are the size of a CB, which we find in the size of nanopores as pointed out above, and the correlation length describing phase coupling or the size of synchronized CB domains. In any CB related dissolution event at a pore tip, a patch of the semiconductors with lateral extension given by this domain size is removed during the active part of a CB cycle. It follows that pores with a diameter much smaller than a domain size cannot exist or are at least not stable. On the other extreme, pores with diameters much larger than a domain size must have several uncorrelated domains working in parallel. “Best” pores are obtained if pore size and domain size are comparable. It follows that if the pore size is a free parameter of the system, it might be expected to scale with the domain size. The domain size in turn, scales with what we have loosely termed the “oxidation strength” of the electrolyte. This is exactly what is observed in certain instances of pore growth (cf. Fig. 14).

Moreover, the observation that two, or on occasion four pores, grow from one nucleus (32, 33) is fully consistent with this picture.

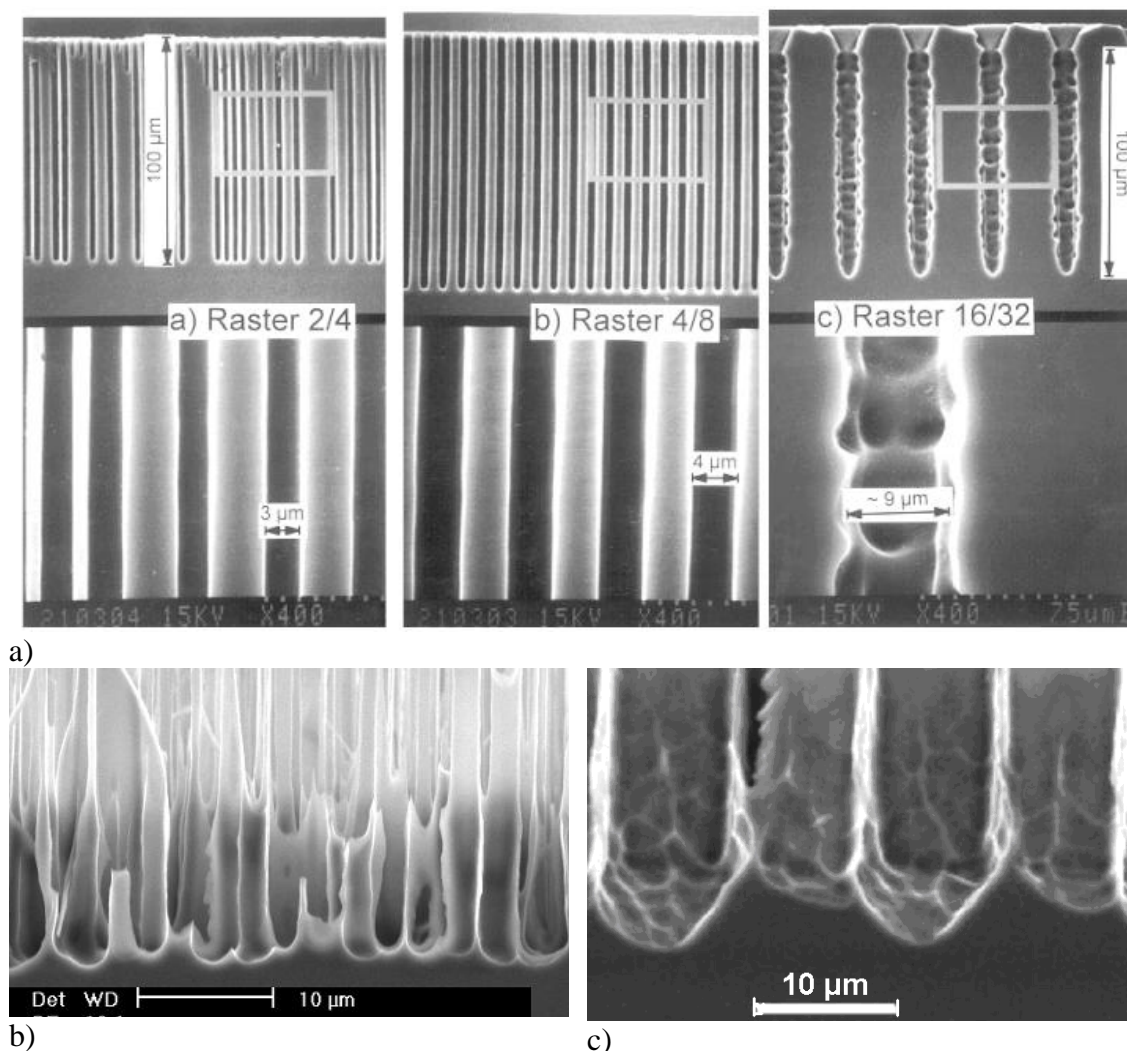


Fig. 14 a) Macropores in n-type Si (seeded by lithography) with (left to right) nuclei distance too small (some pores stop growing, the other increase in size), just right, and too large (bumpy pores). b) Macropores in p-type Si nucleated randomly (pore size \approx domain size) and c) by lithography at a distance much larger than a domain size. The pores in c) grow with diameters larger than a domain size. The bumps on the pores clearly reflect the domain size in both cases

5. Conclusions and Outlook

Anodically etched pores in semiconductors come in all sizes and shapes. Geometries range from nanopores to macropores with diameters beyond $10\ \mu\text{m}$, morphologies include fractal patterns, sponges, straight pore arrays, and self-organized three-dimensional pore crystals. In addition, the crystal symmetry may be expressed in many ways including rather peculiar ones or not at all. It is very clear that no “simple” theory will be able to describe all of this by just looking at diffusion-controlled chemical reactions. This is emphasized by the observation that pores in different semiconductors nevertheless share an increasing number of key properties that obviously cannot be tied to a chemical context alone.

The CB model provides a new paradigm that is to some extent independent of the detailed chemistry. It is particularly suited to the modeling of self-organization features because it contains the essential ingredients like stochastic events, intrinsic time and length scales, and mechanisms that lead to correlations in space and time. At present, some features of the dissolving semiconductor electrode have been quantitatively reproduced in large detail while others are only addressed qualitatively. Nevertheless it is clear that the CB model is capable of providing a framework that allows addressing many of the relevant pore etching questions in a systematic and consistent way. Moreover, as shown here, the CB model has some predictive power and has already been successfully used to produce new pore structures.

It remains to develop the model further and to fit it to specific systems. While the focus is still on semiconductors, we expect that the CB model will eventually also be able to describe the pore formation during anodic oxidation of valve metals like Ti or Al since many of its pertinent features can be recognized in the experimental data published on this topic.

Acknowledgements

The authors are indebted to many researchers who contributed substantially to the development of the model. Particularly helpful was the work of Drs. M. Christophersen, A. Cojocar, E. Foca, S. Frey, G. Hasse, S. Langa, M. Leisner, and S. Rönnebeck. Many discussions with our late friends U. Gösele and V. Lehmann are fondly remembered, as are the contributions and constructive criticisms of Drs. J.-N. Chazalviel, J. Grzanna, K. Krischer, H.J. Lewerenz and I.M. Tiginyanu.

References

1. H. Föll, M. Leisner, A. Cojocar, and J. Carstensen, *Electrochim. Acta* **55**(2), 327 (2009).
2. V. Lehmann, *Electrochemistry of Silicon*, Wiley-VCH, Weinheim (2002).
3. E. Foca, J. Carstensen, G. Popkirov, and H. Föll, *ECS Trans.* **6**(2), 345 (2007).
4. J.-N. Chazalviel, F. Ozanam, M. Etman, F. Paolucci, L.M. Peter, and J. Stumper, *J. Electroanal. Chem.* **327**, 343 (1992).
5. J. Grzanna, H. Jungblut, and H.J. Lewerenz, *J. Electroanal. Chem.* **486**, 190 (2000).
6. K. Krischer and H. Varela, in: *Handbook of Fuel Cells*, ed. by W. Vielstich, A. Lamm and H. Gasteiger, John Wiley & Sons, Ltd **2**(6), 679 (2003).
7. E. Foca, J. Carstensen, and H. Föll, *J. Electroanal. Chem.* **603**, 175 (2007).
8. S. Langa, J. Carstensen, I.M. Tiginyanu, M. Christophersen, and H. Föll, *Electrochem. Solid-State Lett.* **4**(6), G50 (2001).
9. E. Harvey, D.N. Buckley, and S.N.G. Chu, *Electrochem. and Sol. State. Lett.* **5**(4), G22 (2002).
10. C. O'Dwyer, D.N. Buckley, and S.B. Newcomb, *J. Electrochem. Soc.* **21**(18), 8090 (2005).
11. A.M. Gonçalves, L. Santinacci, A. Eb, I. Gerard, C. Mathieu, and A. Etcheberry, *Electrochem. Solid-State Lett.* **10**(4), D35 (2007).

12. Y.H. Ogata, T. Itoh, M.L. Chourou, K. Fukami, and T. Sakka, *ECS Trans.* **16(3)**, 181 (2008).
13. K. Krischer, "Nonlinear dynamics in electrochemical systems, Volume 8", in *Advances in electrochemical science and engineering*, eds. R.C. Alkire and D.M. Kolb, 89, Wiley-VCH, Weinheim (2003).
14. J.-N. Chazalviel and F. Ozanam, *ECS Trans.* **16(3)**, 189 (2008).
15. S. Langa, I.M. Tiginyanu, J. Carstensen, M. Christophersen, and H. Föll, *Appl. Phys. Lett.* **82(2)**, 278 (2003).
16. J. Grzanna, H. Jungblut, and H.J. Lewerenz, *J. Electroanal. Chem.* **486**, 181 (2000).
17. J. Grzanna, H. Jungblut, and H.J. Lewerenz, *Phys. Stat. Sol. (a)* **204(5)**, 1245 (2007).
18. X.G. Zhang, *Electrochemistry of silicon and its oxide*, Kluwer Academic - Plenum Publishers, New York (2001).
19. M. Christophersen, J. Carstensen, and H. Föll, *Phys. Stat. Sol. (a)* **182(1)**, 45 (2000).
20. H. Föll, M. Christophersen, J. Carstensen, and G. Hasse, *Mat. Sci. Eng. R* **39(4)**, 93 (2002).
21. V. Lehmann and U. Gösele, *Appl. Phys. Lett.* **58(8)**, 856 (1991).
22. H. Föll, S. Langa, J. Carstensen, S. Lölkes, M. Christophersen, and I.M. Tiginyanu, *Adv. Mater.* **15(3)**, 183 (2003).
23. M. Leisner, J. Carstensen, and H. Föll, *ECS Trans.* **19(3)**, 321 (2009).
24. M. Leisner, J. Carstensen, and H. Föll, *Nanoscale Res. Lett.* **5(7)**, 1190 (2010).
25. S. Langa, J. Carstensen, I.M. Tiginyanu, M. Christophersen, and H. Föll, *Electrochem. and Solid State Lett.* **5**, C14 (2002).
26. E. Spiecker, M. Rudel, W. Jäger, M. Leisner, and H. Föll, *Phys. Stat. Sol. (a)* **202(15)**, 2950 (2005).
27. I.M. Tiginyanu, V.V. Ursaki, E. Monaico, E. Foca, and H. Föll, *Electrochem. and Sol. State Lett.* **10(11)**, D127 (2007).
28. C. O'Dwyer, D.N. Buckley, D. Sutton, and S.B. Newcomb, *J. Electrochem. Soc.* **153(12)**, G1039 (2006).
29. H. Föll, J. Carstensen, M. Christophersen, and G. Hasse, *Phys. Stat. Sol. (a)* **182(1)**, 7 (2000).
30. S. Matthias and F. Müller, *Nature* **424**, 53 (2003).
31. H. Föll, M. Leisner, J. Carstensen, and P. Schauer, *ECS Trans.* **19(3)**, 329 (2009).
32. E.V. Astrova and A.A. Nechitailov, *Phys. Stat. Sol. (a)* **206(6)**, 1235 (2009).
33. X.Q. Bao, J.W. Jiao, Y.L. Wang, K.W. Na, and H. Choi, *J. Electrochem. Soc.* **154(3)**, D175 (2007).